Paradoxical buffering of calcium by calsequestrin demonstrated for the calcium store of skeletal muscle

Leandro Royer,[1] Monika Sztretye,[1] Carlo Manno,[1] Sandrine Pouvreau,[1] Jingsong Zhou,[1] Bjorn C. Knollmann,[2] Feliciano Protasi,[3] Paul D. Allen,[4] and Eduardo Ríos[1]

[1]Section of Cellular Signaling, Department of Molecular Biophysics and Physiology, Rush University, Chicago, IL 60612
[2]Department of Medicine and Pharmacology, Vanderbilt University, Nashville, TN 37240
[3]Centro Scienze dell'Invecchiamento, Università G. d'Annunzio, 66100 Chieti, Italy
[4]Department of Anesthesia, Perioperative and Pain Medicine, Brigham and Women's Hospital, Harvard Medical School, Boston, MA 02115

Contractile activation in striated muscles requires a Ca^{2+} reservoir of large capacity inside the sarcoplasmic reticulum (SR), presumably the protein calsequestrin. The buffering power of calsequestrin in vitro has a paradoxical dependence on $[Ca^{2+}]$ that should be valuable for function. Here, we demonstrate that this dependence is present in living cells. Ca^{2+} signals elicited by membrane depolarization under voltage clamp were compared in single skeletal fibers of wild-type (WT) and double (d) Casq-null mice, which lack both calsequestrin isoforms. In nulls, Ca^{2+} release started normally, but the store depleted much more rapidly than in the WT. This deficit was reflected in the evolution of SR evacuability, *E*, which is directly proportional to SR Ca^{2+} permeability and inversely to its Ca^{2+} buffering power, *B*. In WT mice *E* starts low and increases progressively as the SR is depleted. In dCasq-nulls, *E* started high and decreased upon Ca^{2+} depletion. An elevated *E* in nulls is consistent with the decrease in *B* expected upon deletion of calsequestrin. The different value and time course of *E* in cells without calsequestrin indicate that the normal evolution of *E* reflects loss of *B* upon SR Ca^{2+} depletion. Decrement of *B* upon SR depletion was supported further. When SR calcium was reduced by exposure to low extracellular $[Ca^{2+}]$, release kinetics in the WT became similar to that in the dCasq-null. *E* became much higher, similar to that of null cells. These results indicate that calsequestrin not only stores Ca^{2+}, but also varies its affinity in ways that progressively increase the ability of the store to deliver Ca^{2+} as it becomes depleted, a novel feedback mechanism of potentially valuable functional implications. The study revealed a surprisingly modest loss of Ca^{2+} storage capacity in null cells, which may reflect concurrent changes, rather than detract from the physiological importance of calsequestrin.

INTRODUCTION

In mammalian skeletal muscle cells, ~200 µmoles of Ca^{2+} per liter of myoplasm are rapidly released from the SR after an action potential to start the signaling process required for muscle contraction (Pape et al., 1993; Baylor and Hollingworth, 2003). This amount constitutes 10–20% of the total Ca^{2+} that can be released from the storage organelle, which is estimated at between 0.7 and 5 mmoles per liter of myoplasm. More details and references for these measures can be found in a recent review (Royer and Ríos, 2009).

Ca^{2+} is released from the SR, an organelle that in fast-twitch mammalian muscle fibers occupies only 5.5% of the total cell volume (Eisenberg, 1984), or 13 times less volume than the accessible myoplasm. To account for the total releasable amount, the total concentration of the ion in the SR at rest must therefore be between 9 and 65 mM.

The concentration of free Ca^{2+} inside the resting SR of skeletal muscle has been measured at 0.35 mM in the frog (Launikonis et al., 2005) or 0.31 mM in the mouse (Rudolf et al., 2006). Based on these figures, the buffering power of the SR, the ratio between total and free $[Ca^{2+}]$, must be between 26 and 200, which requires a buffer of large capacity inside the SR. To meet the requisite of fast delivery, the reservoir must not have a high Ca^{2+}-binding affinity and should be far from saturated at the physiological $[Ca^{2+}]_{SR}$. These demands are ideally met by the protein calsequestrin, which since its discovery nearly 40 years ago is seen as the main provider of functional Ca^{2+}-binding sites within the SR (MacLennan and Wong, 1971; Donoso et al., 1995; Murphy et al., 2009).

L. Royer and M. Sztretye contributed equally to this paper.
Correspondence to Eduardo Ríos: erios@rush.edu
L. Royer's present address is Institut Francois Magendie, INB, 33077 Bordeaux, France.
S. Pouvreau's present address is Physiologie Intégrative Cellulaire et Moléculaire, Université Claude Bernard Lyon 1, 69622 Villeurbanne, France.

Abbreviations used in this paper: FDB, flexor digitorum brevis; *NFRC*, normalized flux rate of change; WT, wild type.

© 2010 Royer et al. This article is distributed under the terms of an Attribution–Noncommercial–Share Alike–No Mirror Sites license for the first six months after the publication date (see http://www.rupress.org/terms). After six months it is available under a Creative Commons License (Attribution–Noncommercial–Share Alike 3.0 Unported license, as described at http://creativecommons.org/licenses/by-nc-sa/3.0/).

The Rockefeller University Press $30.00
J. Gen. Physiol. Vol. 136 No. 3 325–338
www.jgp.org/cgi/doi/10.1085/jgp.201010454

The Journal of General Physiology

Downloaded from http://rupress.org/jgp/article-pdf/136/3/325/1788585/jgp_201010454.pdf by guest on 09 February 2026

In addition to this reversible buffer role, there is evidence in cardiac muscle of a function of calsequestrin as intra-SR Ca^{2+} "sensor," mediating a two-way modulation by $[Ca^{2+}]_{SR}$ considered essential for termination of Ca^{2+} release (Cheng and Lederer, 2008; Qin et al., 2008; Domeier et al., 2009). The interest in these effects is both fundamental and translational, as grave diseases affecting cardiac rhythm have been associated with deficits of termination of Ca^{2+} release and inheritable mutations of cardiac calsequestrin (Terentyev et al., 2003; Knollmann et al., 2006; Györke and Terentyev, 2008; Valle et al., 2008; Liu et al., 2009).

In contrast, a comparable calsequestrin function of control of RYRs has not been clearly demonstrated for skeletal muscle (for review see Ríos et al., 2006). Although Wang et al. (2006) found that lumenal-side Casq1 enhanced the activity of RYR1 channels derived from C_2C_{12} muscle myotubes silenced for both Casq isoforms, bilayer studies comparable to those that demonstrated modulation of cardiac RYRs (Qin et al., 2008) found no effect of either Casq isoform on RYR1 channels (Qin et al., 2009). Additionally, in isolated muscle cells large store depletion increases channel openness (Launikonis et al., 2006), an effect opposite that observed in the heart.

It is therefore unlikely that calsequestrin alters the gating of release channels in skeletal muscle as it does in cardiac muscle. In contrast, the importance of calsequestrin 1 as buffer has found recent confirmation, both from the demonstration of smaller Ca^{2+} transients in the Casq1-null mouse (Paolini et al., 2007) and by a good correlation between calsequestrin content and maximal SR calcium content in rat muscles (Murphy et al., 2009).

The buffering function is especially interesting in skeletal muscle, not just because of a much greater SR content of total calcium and consequent need for buffering power, but because the buffer inside the skeletal muscle calcium store may have unique properties.

To establish basic nomenclature, we define "buffering power" of a Ca^{2+}-binding molecule or an organelle like the SR as

$$B \equiv {[Ca]_T}\Big/{[Ca^{2+}]}, \tag{1}$$

where $[Ca^{2+}]$ is the free concentration and $[Ca]_T$ is the total concentration bound to the molecule or inside the SR. Additionally the "differential" or "slope" buffering power is

$$b \equiv {d[Ca]_T}\Big/{d[Ca^{2+}]}. \tag{2}$$

For a simple 1:1, ligand L, B, and b become equal and reach their maximum precisely at $[Ca^{2+}] = 0$, as can be seen trivially by differentiation of

$$[Ca:L] = {[Ca^{2+}][L]_T}\Big/{\left([Ca^{2+}] + K_D\right)}, \tag{3}$$

an equation representing what we will refer to as "linear buffering." Linear buffering is therefore characterized by a decreasing dependence of B and b on $[Ca^{2+}]_{SR}$.

The evidence that the SR has unique buffering properties was reviewed recently (Royer and Ríos, 2009). It includes the demonstration of nonlinear overall buffering by skeletal muscle SR (whereby B increases with $[Ca^{2+}]_{SR}$ rather than decrease as expected; Pape et al., 2007) and paradoxical behavior of calsequestrin in solution (Park et al., 2003, 2004), whereby b not only increases, but also makes discrete jumps as $[Ca^{2+}]$ is raised. Another indication of a special role is in the elaborate polymeric arrangement of calsequestrin molecules inside terminal cisternae (see, for instance, images by C. Franzini-Armstrong and S. Boncompagni in Fig. 1 of Royer and Ríos, 2009), which has led to speculations of a role as "calcium wires," conduits that deliver calcium to the lumenal mouth of the release channels (MacLennan and Reithmeier, 1998). Finally, the evidence includes surprising findings that remain unexplained: the continuing decay of $[Ca^{2+}]_{SR}$ after sparks terminate (Launikonis et al., 2006), a paradoxical increase in $[Ca^{2+}]_{SR}$ imaged in frog fibers releasing Ca^{2+} (Launikonis et al., 2006) and an analogous rise in lumenal $[Ca^{2+}]$ that precedes pharmacologically induced release from SR vesicles (Ikemoto et al., 1989). All of these observations can loosely be understood assuming that calsequestrin engages in dynamic changes in its state of aggregation as $[Ca^{2+}]_{SR}$ varies, and that these changes in turn alter the protein's buffering power.

The present work was undertaken to determine the extent of the buffer role of calsequestrin in muscle, and search for the putative paradoxical $[Ca^{2+}]$-dependent changes in its buffering power. The strategy was to measure in single voltage-clamped cells of fast-twitch muscle Ca^{2+} release flux in conditions that lead to SR depletion, including prolonged depolarization (which changes SR content as it proceeds) and exposure to a Ca^{2+}-free solution (which changes the resting SR load). The changes induced by these operations were compared with the effects of the complete absence of calsequestrin, as observed in a mouse engineered to lack both calsequestrin 1 and 2 isoforms. We found that Ca^{2+} release in fibers devoid of calsequestrin is strikingly similar to that recorded in the wild type (WT) after SR depletion. Put another way, when the SR Ca^{2+} concentration is low, the SR works as if it had little or no calsequestrin.

MATERIALS AND METHODS

Transgenic animals

Mice lacking both Casq1 and 2 were produced by breeding the Casq1-null (Paolini et al., 2007) and Casq2-null lines (Knollmann et al., 2006). The animals, raised at Charles River Laboratories,

Downloaded from http://rupress.org/jgp/article-pdf/136/3/325/1788585/jgp_201010454.pdf by guest on 09 February 2026

were shipped to the animal facility of Rush University at 4–8 wk of age.

Isolation of single fibers from adult mice

Protocols using mice were approved by the Institutional Animal Care and Use committee of Rush University, which found them consistent with their ethical standards. The present results were collected from 10 WT and 15 Casq-null mice. Young mice (6–10 wk) of weight, *W*, between 25 and 32 g, were euthanized by CO_2 inhalation. The flexor digitorum brevis (FDB) muscle was dissected in Tyrode's solution, and then transferred to a microcentrifuge tube containing 1 ml of 0.2% collagenase in 0 Ca^{2+} Tyrode's solution and incubated at 37°C in an orbital shaker at 50 rpm for a time equal to 10 min + *W* grams × 1 min/gram. After enzymatic digestion, the muscle was transferred to regular Tyrode's solution and stored at 4°C. Single fibers were obtained by gently passing the FDB muscle through pipettes of different tip sizes.

Electrophysiology

The whole cell patch clamp technique was used to impose voltage control in single FDB mouse fibers. The method used was based on the implementation of Wang et al. (1999). Experiments were performed with an Axopatch 200 B amplifier (Axon Instruments) at room temperature. Data acquisition, pulse generation, and synchronization with confocal imaging were performed by a computer running custom software.

Pipettes were pulled from borosilicate glass capillaries (Harvard Apparatus) using a vertical micropipette puller (PC-10; Narishige). The pipettes were heat-polished under microscope observation to a tip diameter of 3–4 µm. The external solution (see Solutions) was based on tetraethylammonium methanesulfonate and contained inhibitors for the sodium (tetrodotoxin) and potassium channels (4-aminopyridine), and blockers of the L-type calcium channel (Cd^{2+} and La^{3+}). The internal solution was based on *N*-methylglucamine glutamate. The substitution of impermeant ions for permeant ones and the presence of inhibitors and blockers allowed a good voltage control of the muscle fiber, documented by Royer et al. (2008). In the set of experiments designed to deplete the SR of Ca^{2+}, fibers were immersed in a solution with 10 µM [Ca^{2+}] and no calcium channel blockers.

Single muscle fibers were dissociated from FDB muscles and transferred to glass coverslip bottom Petri dishes as described above. Fibers were patched near their center and clamped at −80 mV. The series resistance was analogically compensated and had a typical value of ∼2–3 MΩ. The holding current ranged from 1 to 10 nA in different fibers and had a typical value of 2 nA. In ∼60% of the cells where Ca^{2+} transients were imaged under voltage clamp, a standard study of intramembranous charge movement was performed. Nonlinear capacitive and ionic currents were obtained by scaled subtraction of currents in control hyperpolarizing pulses to −100 mV, which were also used to evaluate C_m. Nonlinear or "intramembranous" capacitive currents, $I_Q(t)$, were obtained by subtracting from the asymmetric current a sloping baseline fitted starting 40 ms after the beginning or the end of the pulse for ON and OFF, respectively. Intramembranous charge transfers Q_{ON} and Q_{OFF} were calculated as the time integral of $I_Q(t)$ during the respective transient, and are expressed normalized by C_m. Q_{ON} versus V_m data were fitted with the Boltzmann function:

$$Q_{ON} = \frac{Q_{max}}{1 + e^{-(V_m - V_t)/K}}, \tag{4}$$

where Q_{max} is the maximum charge transfer, V_t is the midpoint (or transition) voltage, and *K* is the voltage change for e-fold increase at limiting low V_m (or steepness factor).

In the experiments designed to deplete the SR, no Ca^{2+} channel blockers were present in the external solution. The control of voltage was good, as judged by the homogeneity of Ca^{2+} transients, but large ionic currents precluded the measurement of intramembranous charge movement.

Solutions

Tyrode's solution contained (in mM): 140 NaCl, 5 KCl, 2.5 $CaCl_2$, 2 $MgCl_2$, and 10 HEPES; pH was set to 7.2 with NaOH and osmolality to 320 mOsm with NaCl. External "reference" contained: 140 mM TEA-CH_3SO_3, 1 mM $CaCl_2$, 3.5 mM $MgCl_2$, 10 mM HEPES, 1 µM TTX (citrate), 1 mM 4-aminopyridine, 0.5 mM $CdCl_2$, 0.3 mM $LaCl_3$, and 25 µM *N*-benzyl-*p*-toluenesulfonamide (BTS; Sigma-Aldrich). External "0 Ca" contained: 140 mM TEA-CH_3SO_3, 0.01 mM $CaCl_2$, 3.5 mM $MgCl_2$, 10 mM HEPES, 1 µM TTX, 1 mM 4-aminopyridine, and 25 µM BTS. In both external solutions, pH was adjusted to 7.2 with TEA-OH and osmolality to 320 mOsm with TEA methanesulfonate. Internal (in pipette) solution contained: 110 mM *N*-methylglucamine, 110 mM liter-glutamic acid, 10 mM EGTA, 10 mM Tris, 10 mM glucose, 5 mM sodium ATP, 10 mM PC Tris, 1 mM free Mg^{2+}, and 100 nM free Ca^{2+}; pH was set to 7.2 with NaOH and osmolality to 320 mOsm with NMG-glutamate.

Confocal imaging and determination of free [Ca^{2+}]

Isolated cells were studied at room temperature in a plastic chamber with coverslip bottom and mounted on a confocal microscope (SP2 AOBS; Leica). Ca^{2+} transients under voltage clamp were derived from line scan images of the fluorescence of rhod-2, introduced through the pipette. Fluorescence of rhod-2 was imaged under excitation at 543 nm ("*Ex*"), collecting light of intensity, *F*, emitted between 562 and 666 nm ("*Em*") at 0.13–0.24-µm pixel intervals and line frequency variable between one every 2.5 ms and one every 5 ms. All line scan images consist of 512 lines.

In all cases, the scanning was parallel to the fiber axis, no more than 10 µm above the bottom surface of the cell. Line scans of voltage-clamped fibers were normalized by the average $F_0(x)$ of $F(x,t)$ during times before the pulse. A line-averaged $F(t)/F_0$ is calculated by averaging over the *x* coordinate in the entire *x* extent of the image. Average cytosolic [Ca^{2+}] (*t*) is derived from $F(t)$ as

$$[Ca^{2+}]_{cyto}(t) = [Ca^{2+}]_{cyto}(0)\left(\frac{F(t)}{F_0} + \frac{dF(t)/dt}{k_{OFF\,dye}F_0}\right). \tag{5}$$

This equation assumes that the dye is far from saturation by Ca^{2+}, an assumption justified in our previous work with internal solutions containing 10 mM EGTA. $[Ca^{2+}]_{cyto}(0)$ is assumed equal to that in the pipette (0.1 µM). Cells exposed to 0 Ca are analyzed differently (see The calculation of Ca^{2+} release flux). The value of $k_{OFF\ rhod\text{-}2}$ was set as 100 s^{-1} (as determined by Royer et al., 2008).

Most cells from dCasq-null mice produced Ca^{2+} transients that were spatially homogeneous. In contrast, all three cells studied from one null mouse plus isolated cells from other null mice (for a total of seven or 21% of all cells studied) responded with transients that were heterogeneous, seen in the line scan as segmental regions with different rates of rise, and in some places complete failure to mobilize Ca^{2+}. A similar heterogeneity in release was observed in only 1 of more than 100 WT mice studied in our laboratory. The heterogeneous response could correspond to a comparative weakness in the mutant, which makes its cells more susceptible to damage by the enzymatic treatment. Alternatively, it might reflect some of the structural abnormalities of plasma and t-tubular membrane described in the Casq1-null mouse by Paolini et al. (2007). Two examples of heterogeneous transients are presented in Fig. S1 B, as these observations might be of interest in further studies of the null animals. Only cells with homogeneous transients were included in the images and analyses of this paper.

Downloaded from http://rupress.org/jgp/article-pdf/136/3/325/1788585/jgp_201010454.pdf by guest on 09 February 2026

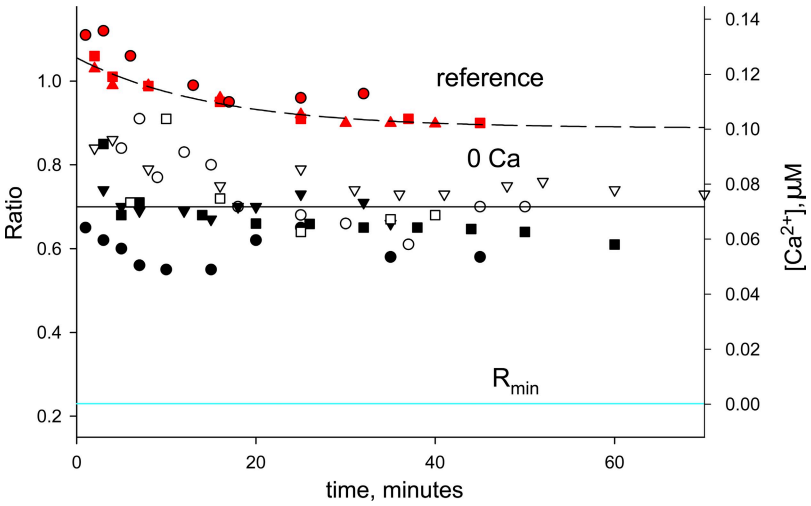

Figure 1. Cytosolic $[Ca^{2+}]$ in different external solutions. Area-averaged ratio of fluorescence of indo-1 in patched cells immersed in reference external solution (red) or in 0 Ca (black) versus time after breaking into the cell. The dashed curve in black is an exponential fit. The continuous black line marks the average for cells in 0 Ca and in cyan is R_{min}, measured in situ, in cells exposed to a Ca^{2+}-free solution, with membrane permeabilized by saponin. Individual cells are identified by different symbols. ID: red, 032910a, b, d; black, 0325a, c, d; black, 0330a, b, c.

The calculation of Ca^{2+} release flux

Ca^{2+} release flux $\dot{R}(t)$ was derived from $[Ca^{2+}](t)$ by a simplified version of the removal method (Melzer et al., 1984; Schuhmeier and Melzer, 2004; Royer et al., 2008). As explained before, in the presence of a high concentration of EGTA, the result of this calculation depends only on the OFF rate constant of the dye and four other parameters. As discussed in detail in previous work, if the choice of parameter values results in a good fit, the kinetics of release flux will be robustly determined, while the scale of the records will remain dependent on parameter values. To make the scale of the results comparable across all fibers, we used the same values of all parameters, except k_{uptake}, the rate constant of Ca^{2+} transport into the SR, which was set for optimal fit of the evolution of $[Ca^{2+}](t)$. $[Dye]_{total}$ and $[EGTA]_{total}$ were set to 0.7 of the concentrations in the pipette (as first done by Ursu et al., 2005). When the experiments lasted more than 60 min, $[Dye]_{total}$ and $[EGTA]_{total}$ were set to 0.9 at this time and interpolated linearly. Other options for the time course of $[EGTA]_{total}$, including exponential entry and a constant value, were tried alternatively, but the quantitative changes that resulted did not require modifying any qualitative conclusions. k_{ON} EGTA was 10 $(\mu M\ s)^{-1}$ and k_{OFF} EGTA was 5 s^{-1}.

Net flux and net amount released

Net flux $\dot{R}_{net}(t)$, positive if leaving the SR, is the difference between release flux and uptake by the SR:

$$\dot{R}_{net}(t) = \dot{R}(t) - k_{uptake} \times [Ca^{2+}]_{cyto}. \quad (6)$$

The amount of Ca^{2+} released at time t is

$$R(t) = \int_0^t \dot{R}_{net}(u)\,du, \quad (7)$$

where zero time is the start of the pulse. $R(t)$ normally grows asymptotically to a maximum, $R(\infty)$, which defines the total amount of Ca^{2+} releasable by depolarization.

It should be kept in mind that the best-fit value of k_{uptake} is correlated near proportionally to the assumed value of [EGTA]total, as is the scale of the resulting calculated flux. Therefore $\dot{R}$, $\dot{R}_{net}$, and $R(\infty)$ remain affected by an unknown scale factor.

Evacuability as metric of SR properties

It has been long recognized that the concentration gradient driving release flux is variable, so that flux per se is not a good indicator of the state of the release channels. A better measure is the "depletion–corrected flux," defined by Schneider et al. (1987) as

$$\dot{R}_c \equiv \frac{\dot{R}}{Ca_{SR}(0) - R(t)}, \quad (8)$$

where the initial SR calcium content, $Ca_{SR}(0)$, was equated to $R(\infty)$.

Since its introduction, $\dot{R}_c$ has been used as a measure of SR channel permeability. Royer et al. (2008) demonstrated that

$$\dot{R}_c = \varphi \frac{P}{B} \equiv E, \quad (9)$$

where P is permeability, defined as flux per unit area and unit concentration gradient, φ is SR area to volume ratio, and B was defined in Eq. 1.

This equation implies that $\dot{R}_c$ does not reflect just channel permeability. Royer et al. (2008) named it evacuability, E, to

TABLE I

Properties of intramembranous charge movement in dCasq-null fibers

		Q_{max} nC/μF	K mV	V_t mV	n cells
dCasq-null	AVG	36.8	9.41	−15.6	10
	SEM	2.72	0.43	1.62	
WT	AVG	39.2	10.9	−18.8	7
	SEM	2.80	0.79	1.43	

Entries are best-fit parameter values of the Boltzmann function (Eq. 1) fitted to Q_{ON} versus V_m data. The last two rows correspond to seven fibers from FDB of reference mice studied by Royer et al. (2008). The differences between averages are not significant.

Downloaded from http://rupress.org/jgp/article-pdf/136/3/325/1788585/jgp_201010454.pdf by guest on 09 February 2026

stress that its value emerges from several properties that together determine the rate or ease with which the SR can be emptied.

Because Ca_{SR} is strictly unknown, E can only be approximated. In the present work, we use the normalized flux rate of change (*NFRC*), defined as

$$NFRC \equiv -\frac{d\dot{R}/dt}{\dot{R}_{net}}, \tag{10}$$

which satisfies the following equality:

$$NFRC = \frac{\varphi P}{B} - \frac{\dot{R}}{\dot{R}_{net}}\frac{d\ln(\varphi P/B)}{dt}. \tag{11}$$

As shown by Royer et al. (2008), the negative "error" term in Eq. 11 is small, provided that two conditions are met: $\dot{R}_{net}$ must not be small, and E (and by extension the *NFRC*) cannot be varying rapidly. Royer et al. (2008) showed with examples that these conditions exclude the first 5–10 ms of a depolarization-induced Ca^{2+} transient (when the *NFRC* is changing very rapidly) and are met during the following 200–250 ms. During this interval, the *NFRC* is a good measure of E.

As defined, E is a generalization of the exponential rate constant of evacuation of the organelle. Thus, if the SR emptied with constant P and B, both its free and total [Ca] would decay exponentially, with rate constant E, and so would the flux. A non-exponential decay with a "shoulder," characteristic of WT cells, results in an increasing E.

Cytosolic free [Ca^{2+}] upon exposure to "0 Ca"

A set of experiments aimed at quantifying the effects of SR depletion on release flux and evacuability was performed. Depletion was achieved by exposing cells to 0 Ca external solution. Because the monitor used to image Ca^{2+} transients, rhod-2, is not ratiometric, resting free cytosolic [Ca^{2+}], $[Ca^{2+}]_{cyto}(0)$, had to be determined to convert the monitor's fluorescence to a [Ca^{2+}] measure (Eq. 5). This was done for both conditions, reference and 0 Ca, in multiple cells using SEER of indo-1 (Launikonis et al., 2005) for a ratiometric measure of $[Ca^{2+}]_{cyto}$. The results are shown in Fig. 1, where different symbols identify individual cells. In cells exposed to reference external solution (red), the cell-averaged ratio tended to a value that was taken to be equal to [Ca^{2+}] in the pipette solution, 100 nM. For cells exposed to 0 Ca before patching (black), the ratio tended rapidly to a value corresponding on average to a concentration of 72 nM. 100 nM and 72 nm were used, respectively, for all experiments in reference and 0 Ca.

Statistical analysis

Differences of unpaired averages were analyzed, assuming normality of the distributions sampled and equality of standard deviations, by two-tailed Student's t test, with significance threshold at $P < 0.05$.

Online supplemental material

Fig. S1 illustrates heterogeneous Ca^{2+} transients observed in a group of cells. It is available at http://www.jgp.org/cgi/content/full/jgp.201010454/DC1.

RESULTS

The six subsections that follow present the results of two distinct studies. The first is a comparison of the Ca^{2+} transients in response to voltage clamp depolarization in FDB muscle fibers of two types of mice: a reference group

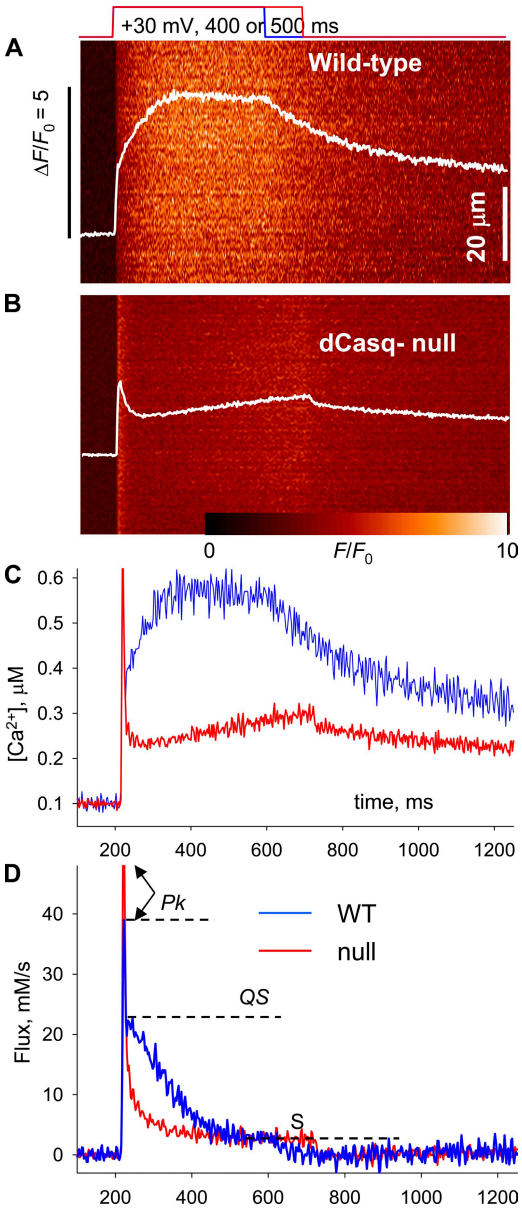

Figure 2. Ca^{2+} transient and release flux in dCasq-null cells. (A and B) Line scan images of fluorescence of rhod-2 normalized to baseline value F_0 (x) in cells (WT or null) subjected to a large, long-lasting depolarization (top). In white is normalized fluorescence averaged over x: $F(t)/F_0$. Note that in the WT, F goes through two stages of growth and plateaus after ~200 ms. In the null example instead, F goes through a sharp peak and then rises steadily without quite reaching a plateau. (C) $[Ca^{2+}]_{cyto}(t)$, derived from $F(t)/F_0$ records in A and B. (D) Release flux $R(t)$ derived from $[Ca^{2+}]_{cyto}$. Three levels of interest are indicated: *Pk*, the value at the early peak of the waveforms; *QS*, a level reached upon descent from the peak and sustained for a brief time in the WT; *S*, a truly steady level reached at ~500 ms in the reference fiber, and, as best seen with the integrals, $R(t)$ (Fig. 7 B), at later times in the dCasq-null. The absence of a *QS* stage and slow decay toward *S* was a consistent observation in the null; the excess in *Pk* was not. Averages of *Pk* and *S* are in Table II. Values of the removal model parameters used in the calculation of flux, which were identical for both cells, are given in Materials and methods. ID: A, 021408a_25; B, 020609b_3.

Downloaded from http://rupress.org/jgp/article-pdf/136/3/325/1788585/jgp_201010454.pdf by guest on 09 February 2026

(WT) and mice null for both calsequestrin isoforms. The second is an examination of the changes in Ca^{2+} transients induced by exposure of cells to an extracellular saline without Ca^{2+}.

The state of the membrane voltage sensor (DHPR) was first evaluated through the properties of their intramembranous charge movement. The linear capacitance, C_m, continuously measured in control currents elicited by voltages negative to the holding potential, was approximately constant during the experiments. Its average, 1.7 nF (SEM 0.22), was not significantly different than the average in WT cells studied by Royer et al. (2008).

Table I lists parameter values for best fit of the Boltzmann function (Eq. 4) to charge transfer Q versus V_m in the ON transients from 10 Casq-null cells. For comparison, the table includes the average parameter values of the WT fibers studied by Royer et al. (2008). There are no significant changes. In summary, the Casq-null cells did not differ substantially from the WT in kinetics, amount, or voltage dependence of their t-tubule voltage sensor charge movement. This statement is valid for the null fibers studied here, selected by exclusion of 21% of cells through criteria described in Materials and methods.

The Ca^{2+} transient of dCasq-null cells

Fig. 2 (A and B) compares confocal line scans of the fluorescence of rhod-2 in a WT FDB cell and a representative cell from a dCasq-null mouse in response to a pulse to a fully activating voltage (+30 mV). The images illustrate consistent differences. In the WT, the fluorescence increases in two stages to a sustained level. As demonstrated by Royer et al. (2008), a 0.4-s pulse is sufficient to cause release of a maximum amount of Ca^{2+} from the SR. In other words, no additional depletion will be caused by pulses of increased voltage or duration. The completion of net release is revealed in the WT case by F reaching a steady or slightly decaying maximum. It is understood that at this point in time, Ca^{2+} release through RYRs becomes balanced by resequestration into the SR (see, for instance, Fig. 6 in Royer et al., 2008).

In the null cells the transient is different. It goes through an initial peak—never seen in the WT—from which it decays rapidly to then recover slowly. In individual null cells, the early peak of fluorescence could reach values greater than in most WT cells at a comparable time during the pulse, a difference that results from a greater initial peak of Ca^{2+} release flux, as described below. This early peak, however, was variable among cells, as reflected in the large standard error of the average (Table II). The recovery of the fluorescence level from the trough that follows the early peak was also variable (for further description of this stage, see Total releasable calcium in Casq-null cells).

The interpretation of the altered kinetics was helped by an analysis of the records in terms of Ca^{2+} release flux, $\dot{R}(t)$. The waveforms of flux are reliable kinetically, although their scale is strictly dependent on the values of the model parameters. In the interest of comparisons across platforms, we assumed values similar to those used in an earlier study (Ursu et al., 2005).

$\dot{R}(t)$ for images in A and B of Fig. 2 is illustrated in panel D. The calculation first derives the line-averaged Ca^{2+} transient ($[Ca^{2+}]_{cyto}(t)$; Fig. 2 C) from the line-averaged fluorescence, taking into account the kinetic constants of the dye. The calculation reveals a sharp difference in $\dot{R}(t)$. As described by Royer et al. (2008), in the WT, $\dot{R}(t)$ goes through an early peak (at a value *Pk*), followed by decay to an intermediate level (*QS*), and then a second fall to a sustained level, *S*. The decay after *QS* was described as a "shoulder." In the null cell, $\dot{R}(t)$ also goes through an initial peak, but then decays in one roughly exponential step, with no shoulder, to the final *S*.

TABLE II

Average properties of release flux

Cell	1	2	3	4	5	6	7
		Pk	*S*	$R(\infty)$	*NFRC*, initial	*NFRC*, final	*n*, cells
		mM/s	*mM/s*	*mM*			
WT	AVG	115	3.07	2.91	6.30	15.2	16
	SEM	5.22	0.51	0.19	0.50	0.51	
dCasq-null	AVG	86.0[a]	2.76	2.34[a]	16.2[a]	5.13[a]	19
	SEM	12.5	0.25	0.17	3.4	1.07	

Two long duration pulses (one of 0.4 or 0.5 s, and the other of 1 s) to +30 mV were applied in every cell and the ensuing Ca^{2+} transients were imaged in line scan mode, respectively, at 2.5 or 5 ms per line. Column 2, peak flux, measured on the transient recorded at 2.5 ms/line and corrected for the blunting effect of low acquisition rate as described by Royer et al. (2008). Column 3, steady flux, reached at variable times into the 1-s pulse. Column 4, total amount of releasable calcium, defined as the asymptotic maximum of the time integral of net flux (compare with Fig. 7). Column 5, *NFRC* value reached immediately after the end of the initial peak of flux; for reference fibers, this was always the minimum value, while in null fibers it was usually the maximum. Column 6, *NFRC* value reached at the end of the interval where it is defined (~250 ms); the *NFRC* value at this time was usually a maximum for reference fibers and a minimum for null fibers (compare with Fig. 3 B).

[a]The value is significantly different from the corresponding value in the WT.

Downloaded from http://rupress.org/jgp/article-pdf/136/3/325/1788585/jgp_201010454.pdf by guest on 09 February 2026

A similar evolution was observed in every image of every null fiber studied. Averaged peak and steady values are compared in Table II. *Pk* was ~20% lower in null cells. *S* did not differ substantially.

SR evacuability was greatly altered in dCasq-null cells

E (Eq. 9) is proportional to *P*, the SR membrane permeability to Ca^{2+}, and inversely to *B*, the SR buffering power for Ca^{2+}. Although *E* is strictly not knowable without direct measurements of SR Ca^{2+}, it can be approximated by the *NFRC* (Eq. 10). Fig. 3 A plots the evolution of the *NFRC* from the flux records in Fig. 2 D. In the WT (blue), this index increases during the pulse, as expected given the shoulder in the flux record (compare Materials and methods). In the Casq-null cell, in contrast, the *NFRC* starts high and decays during the pulse.

That these differences are reproducible is demonstrated in Fig. 3 B, displaying records obtained by averaging the *NFRC* from every available line scan in WT and null animals. Solid and dashed lines correspond to different image acquisition frequencies. A different representation of the same measures is in Table II, listing averages of the extreme values of *NFRC*. Both representations demonstrate the striking effect of the double Casq deletion.

As argued by Royer et al. (2008), the evolution of *E* in the WT may reflect an increase in *P* (hypothesis 1), a decrease in *B* (hypothesis 2), or both changes occurring together. Because in Casq-null cells, which lack the main buffer, *E* started much higher, the results are apparently more consistent with hypothesis 2. Alternatives will be considered in the Discussion.

The result prompts another inference: as can be seen in both Fig. 3 and Table II, the value of *E* attained when the SR has released most of the Ca^{2+} that it can release is similar to the initial value of *E* in the null cells. The Ca-depleted situation recreates in this sense the functional phenotype of the calsequestrin-lacking cells. As recalled in the Introduction, the buffering power of calsequestrin decreases with $[Ca^{2+}]$ in solution. If this property applied in vivo, *B* provided by calsequestrin should decrease as the SR depletes, thus explaining the rise in *E*. The decay of *E* upon release in the nulls is an unexpected additional phenomenon, taken up in the Discussion.

Ca^{2+} transients changed shape at low SR loads

If the increase in *E* during depolarizing pulses in the WT was due to loss of buffering power by calsequestrin in the lower $[Ca^{2+}]$ of a depleted SR, the increase should be reproducible upon depletion by other means. This hypothesis was tested by exposing WT muscle fibers to an external solution, 0 Ca, with only a small amount of Ca^{2+} left (to facilitate patching). As shown later, this exposure resulted in substantial reduction of releasable calcium after tens of minutes.

Fluorescence transients and flux are illustrated in Fig. 4. Compared with the reference (in blue), $F(t)$ in 0 Ca lacked the rise in two phases and resembled instead that of Casq-null cells, with features that included an early peak followed by decay and often a second slow increase. The corresponding flux records are in Fig. 4 B. In this and six other cells studied in the same way, the flux, which started with a peak similar to that in reference, presented in the earliest records a lesser shoulder and evolved upon longer exposure to a seemingly exponential decay.

To better demonstrate the kinetic changes, the flux records of the cell in 0 Ca are shown again in Fig. 4 C,

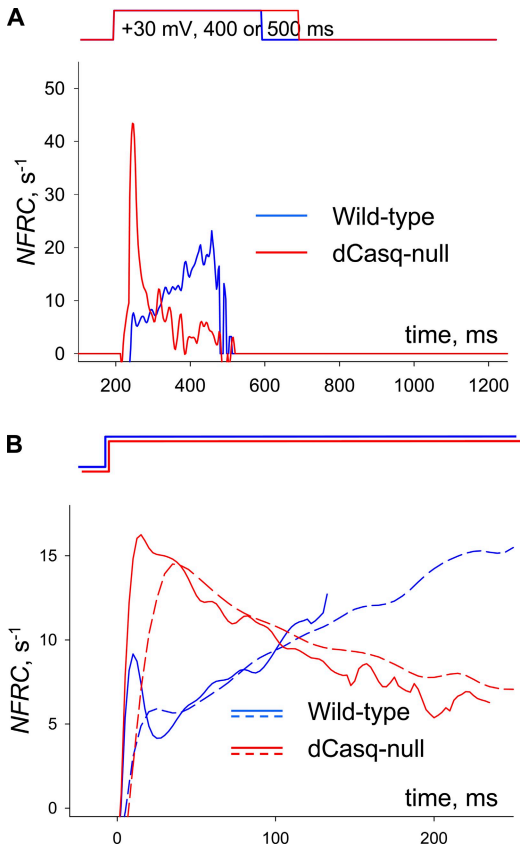

Figure 3. Evolution of evacuability in WT and dCasq-null cells. (A) The *NFRC*, an index approximately equal to *E* (see Materials and methods) calculated for the example images of Fig. 2. The *NFRC* is ill-defined if $\dot{R}_{net}(t)$ is close to zero. We stop its calculation when $\dot{R}_{net}(t)$ reaches a (low) threshold of 1 mM/s, which occurs by ~300 ms in these examples. (B) Averages of $NFRC(t)$ over all WT and null cells subjected to long duration pulses. Two acquisition frequencies were used to allow for different pulse durations in images of the same digital format. For averaging, the traces were grouped by frequency (solid, 2.5 ms/line; dashed, 5 ms/line) and aligned to the beginning of the pulse. Averaging was extended to the first time when $\dot{R}_{net}$ reached threshold in any individual record. Except at the beginning of the pulse, when *NFRC* changes rapidly and is not a good measure of *E* (Materials and methods), the properties of the averages do not depend on scanning frequency. The averages generally reproduce the evolution of the individual examples in A.

Downloaded from http://rupress.org/jgp/article-pdf/136/3/325/1788585/jgp_201010454.pdf by guest on 09 February 2026

smoothed and scaled to the same peak. Superimposed for comparison is $\dot{R}$ of the Casq-null cell image in Fig. 2. In this and other cells, as time in 0 Ca increased, release flux decreased in amplitude, lost its shoulder, and featured a progressively faster decay, becoming similar in kinetics to $\dot{R}$ of Casq-null cells.

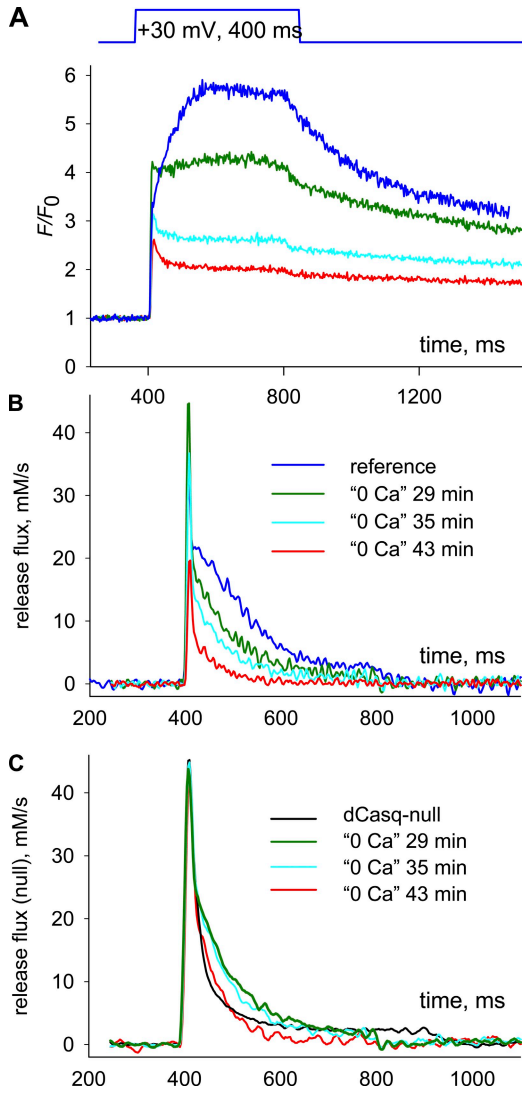

Figure 4. Fluorescence and flux in WT cells exposed to 0 Ca. (A) Fluorescence transients in response to the depolarizing pulse shown. Traces in green, cyan, and red are for the same cell after increasing times of exposure to 0 Ca (keyed in B). The record in blue is from a different cell in reference solution. Note that the amplitude of transients progressively falls and their kinetics becomes increasingly similar to that of the dCasq-null in Fig. 2. (B) $\dot{R}(t)$, calculated from records in A, showing that in 0 Ca records lose the shoulder, characteristic of the WT in reference solution, becoming progressively similar to flux in dCasq-null cells. This is demonstrated in C, where the records in 0 Ca from B are scaled to match the peak of the $\dot{R}(t)$ from the dCasq-null example in Fig. 2. ID: WT in reference, 122206d_26; WT in 0 Ca, 052209b_9, 10, 11. For calculations of flux, [EGTA] in the 0 Ca example was assumed to enter the cell according to a saturating exponential of $\tau = 40$ min.

Evacuability increased at low SR loads

To test the working hypothesis 2—that the increase in E during Ca^{2+} release is due to a reduction in B—it was important to evaluate the changes in E brought about by SR depletion in the WT. This evaluation is illustrated in Fig. 5 on images acquired at greater temporal resolution and

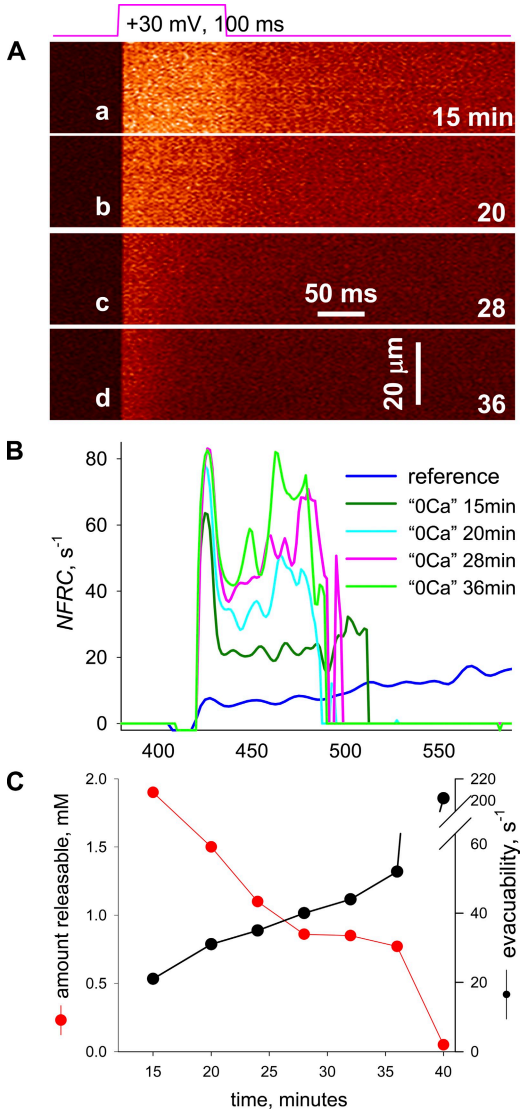

Figure 5. The evolution of evacuability in a cell exposed to 0 Ca. (A) Line scans of fluorescence in a WT cell exposed to 0 Ca. Times of exposure are given, in minutes, at the bottom right corner of every panel. (B) *NFRC* for images in A. In blue is *NFRC* for a WT cell in reference solution (same as in Fig. 2). Images for the cell in 0 Ca were acquired at a higher frequency, hence the initial peak in *NFRC*, which is blunted in the reference record. Although *NFRC* increases with time of exposure, the interval when it is defined becomes shorter, a direct result of the increase in E. (C) Black symbols, evacuability, calculated for images in A and other images as an average of the *NFRC* in the first 20 ms after the initial peak (the initial peak is excluded because a rapidly changing *NFRC* ceases to be a good approximation of E). Red symbols, total releasable amount of calcium, $R(\infty)$, plotted versus time of exposure to 0 Ca. Note the inverse dependence between evacuability and amount releasable. ID, 092409b. Reference is 021408a_25.

Downloaded from http://rupress.org/jgp/article-pdf/136/3/325/1788585/jgp_201010454.pdf by guest on 09 February 2026

summarized for multiple fibers in Fig. 6. Fig. 5 A shows fluorescence changes in response to a high voltage pulse at increasing times in 0 Ca. Fig. 5 B plots *NFRC* for each record. The average *NFRC* in reference solution is added for comparison (record in blue).

A quantitative summary of the experiment is in panel Fig. 5 C, plotting E (black) and releasable amount of calcium, $R(\infty)$ (red), versus time of exposure to 0 Ca. E increased monotonically as the releasable amount decreased.

The inverse relationship between E and $R(\infty)$ applied uniformly across times, loads, and experimental conditions. This is documented in Fig. 6, which summarizes 7 experiments in 0 Ca and 17 in reference external solution, all in WT mice. The continuous line plots the hyperbolic decay that fits best all points.

The conclusion from this section is that E increases monotonically as $R(\infty)$ decreases. The change in E with SR content is thus consistent with the hypothesis that calsequestrin loses buffering power as it loses bound Ca^{2+}. The changes in 0 Ca were, however, not identical to those observed in the dCasq-null muscles. The most interesting divergence was a progressive decrease in E during Ca^{2+} release in the null cells, corresponding to a slow creep upwards in $[Ca^{2+}]_{cyto}$ during the depolarizing pulse. Some WT cells exhibited this evolution when exposed to 0 Ca, but many did not, showing instead an elevated E, constant or increasing during the time that E was measurable (e.g., Fig. 5 B). As argued below, this difference probably reflects changes during development in the null mice, which cannot be reproduced by an acute reduction of SR calcium content. Additional unspecified alterations brought about by the lack of extracellular Ca^{2+} could also explain this difference.

Total releasable calcium in dCasq-null cells

Calsequestrin is believed to be the main buffer of Ca^{2+} inside the SR; therefore, elimination of calsequestrin would be expected to result in severe curtailment of $R(\infty)$, the maximum amount of Ca^{2+} that can be released by depolarization.

The calculation of $R(\infty)$, as the maximum reached asymptotically, upon a long-lasting, high voltage depolarization of the integral of $\dot{R}_{net}(t)$ is illustrated in Fig. 7. $\dot{R}_{net}$ is represented in Fig. 7 A for pulses of 1-s duration in a WT (blue) and a null cell (cyan). Also represented is $\dot{R}_{net}$ calculated for the null cell transient in Fig. 2 B (red). $\dot{R}_{net}$ evolves similarly to $\dot{R}$, but tends to zero after a variable time of depolarization. The corresponding running integrals of flux, $R(t)$, are in Fig. 7 B.

For the WT cell in the figure, $R(t)$ did not climb monotonically, but came down slightly after a maximum. (A reason for the slight decrease, which is also present in the raw fluorescence signal, may be a spatial heterogeneity in control of membrane voltage, which results in greater activation near the pipette.) $R(\infty)$ was taken to be that maximum. For the null cell represented by the curve in cyan, $R(t)$ had not quite reached its maximum by the end of the 1-s pulse, and $R(\infty)$ was calculated as the asymptote of the exponential fit to $R(t)$ in the last 700 ms of the pulse. For the null cell represented by the curve in red, $R(\infty)$ was not defined. The average $R(\infty)$ in all cells where it was defined, listed in Table II, was reduced by 20% in the null fibers, a statistically significant difference.

The kinetic difference demonstrated in the figure is representative of most cells. In WT cells, $R(t)$ always reached its steady value in ~0.5 s or less, a time when $R(t)$ was still increasing in most null cells. 13 of 19 Casq-null cells featured such slow tendency to $R(\infty)$, which of course reflected a slower decay of $\dot{R}_{net}$ to zero (visible in Fig. 7 A).

In a qualitative sense, the kinetic difference does not depend on the assumptions needed to calculate $R(t)$.

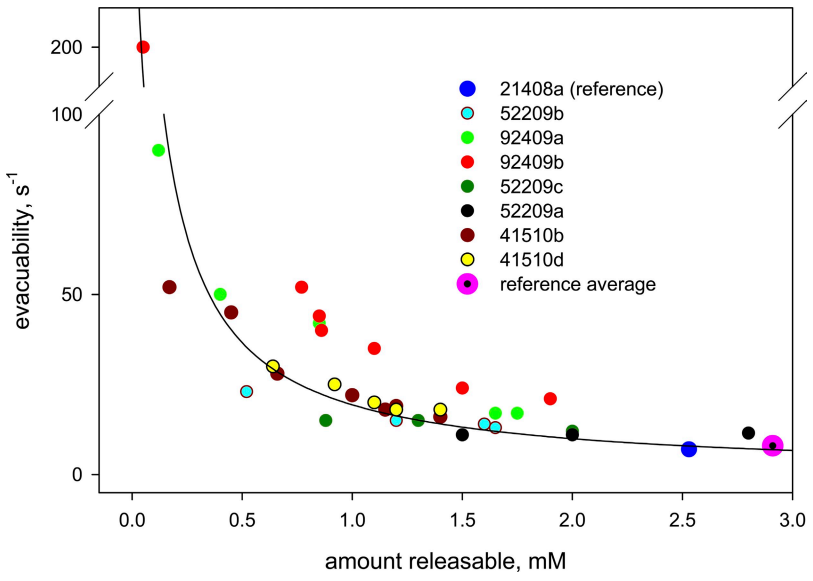

Figure 6. Evacuability is inversely related to releasable amount of calcium in the SR. Symbols plot the initial value of E, calculated by an average of *NFRC* as described in Fig. 5, versus the corresponding $R(\infty)$, calculated on the same or a contemporaneous transient of adequate duration, for individual cells after varying times of exposure to 0 Ca. Colors identify individual cells. The blue circle and the large pink circle represent, respectively, the example WT cell of Fig. 2 and average values for 17 cells in reference solution. The continuous line plots the function $E = ab/(R+b)$, with $a = 334\ mM^{-1}s^{-1}$ and $b = 0.0615$ mM.

Downloaded from http://rupress.org/jgp/article-pdf/136/3/325/1788585/jgp_201010454.pdf by guest on 09 February 2026

Indeed, the evolution of $R(t)$ is roughly proportional to that of F or $[Ca^{2+}]_{cyto}$ because in the highly buffered internal solution used here, the net amount of Ca^{2+} released is translated almost linearly to the final increases in $[Ca^{2+}]$ and fluorescence. The surprising conclusion is, therefore, that when channels are maximally activated by voltage, net release lasts for a longer time in Casq-null than WT cells.

Release flux elicited by trains of pulses

One last aim was to explore the differences due to the absence of calsequestrin using a depolarization closer to the train of action potentials that activates Ca^{2+} release in the living animal. In mouse FDB at body temperature, a typical action potential may have a full duration at half-maximum of 1 ms, whereas the train may have a duration of 1 s and a frequency of 30–120 Hz (unpublished data). To produce a series of resolved Ca^{2+} transients at room temperature, we applied depolarizations at the low end of those frequencies (30 Hz) with the pattern illustrated in Fig. 8 A. Five fibers of each type, null and WT, were subjected to such trains.

The fluorescence transients of one WT and one null fiber are shown in Fig. 8. Ca^{2+} transients are in Fig. 8 C, and $\dot{R}$ is in panel D. The comparison is completed in Fig. 8 E, showing the evolution of the amount released $R(t)$ in the successive depolarizations. The comparisons in Fig. 8 recapitulate qualitatively every observation made using continuous depolarizations. The imaginary line tracing the peaks of $\dot{R}$ features a shoulder for the WT and a faster, exponential-like decay for the null. The differences are also present in the evolution of peak (and average) fluorescence, namely a two-stage increase in the WT, which levels off in hundreds of ms, and an initial peak followed by a trough and a much slower creep upward in the null. The integrated amount released (Fig. 8 E) features similar differences. Although these evolutions take place at a slower pace than with continuous depolarizations, every kinetic aspect of the difference between WT and null seems to be reproduced qualitatively. This result shows that features of responses obtained with continuous depolarization can be extrapolated to the responses to more physiological trains, at least qualitatively.

DISCUSSION

The present work was designed to continue the examination of the processes that in mammalian muscle control Ca^{2+} release from the SR. In particular, it sought answers to questions first raised by Royer et al. (2008) in their study of the response to activating pulses that cause substantial emptying of the SR.

The evolution of evacuability is associated with changes in SR Ca^{2+} buffering

Royer et al. (2008) showed that the flux of Ca^{2+} release activated by a long-lasting depolarization evolves along a complex decay path (demonstrated in Fig. 2 D). Release starts with an initial peak, terminated by a first, abrupt phase of decay. In amphibian muscle, the work of Baylor and Hollingworth (1988), Schneider and Simon (1988), Jong et al. (1995), Pape et al. (1995), and Pizarro and Ríos (2004) ascribed this decay to inactivation mediated by cytosolic Ca^{2+} ("CDI"). This phase is followed by a slower decay, which presents with a "shoulder" that can be described more precisely as a change from negative to positive curvature in $\dot{R}(t)$.

Royer et al. (2008) also showed that this shoulder resulted mathematically in a rising value of E. The increase in E could reflect an increase in P (expected,

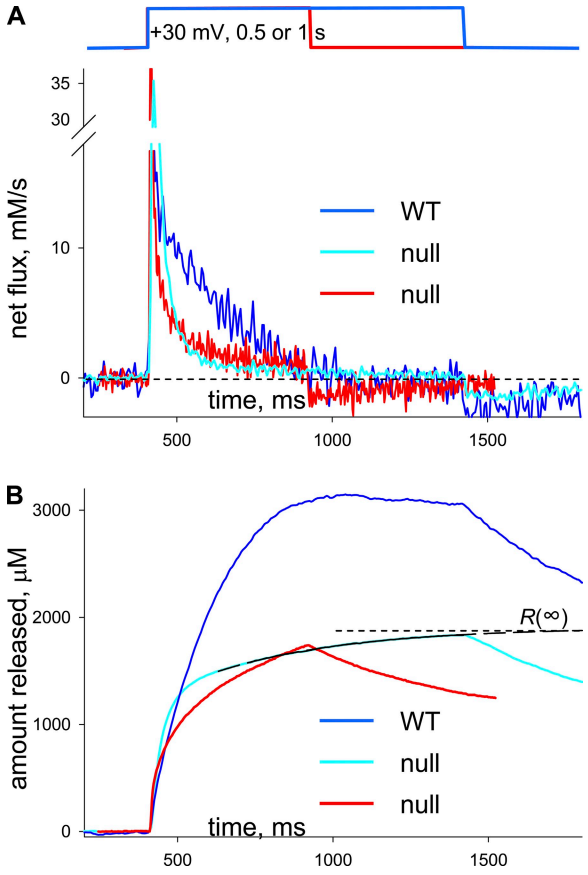

Figure 7. Substantial releasable Ca^{2+} remains in dCasq-null cells. (A) $\dot{R}_{net}(t)$ calculated (Eq. 6) for a WT cell (blue) and a dCasq-null cell (cyan) subjected to a 1-s–long depolarization, and the dCasq-null cell of Fig. 2 (red). $\dot{R}_{net}(t)$ is similar to $\dot{R}(t)$ but tends to 0 during the pulse and becomes negative afterward. It therefore shows similar kinetic differences between WT and null cells. (B) Net amount of Ca^{2+} released, $R(t)$, calculated (by Eq. 7) for the fluxes in A. The records illustrate that null cells may release substantial amounts of calcium (see Table II for averages). They also show that $R(t)$ typically reaches its maximum, $R(\infty)$, much sooner in the WT. For the case represented by the cyan curve, $R(t)$ did not quite reach maximum, and $R(\infty)$ was calculated as the asymptote to the curve in black, an exponential fit to the last 700 ms of $R(t)$ during the pulse. $R(\infty)$ could not be reliably established for the release record represented in red. ID: WT, 101906b_31; nulls, 082108c_14 (cyan) and 020609b_3 (red).

Downloaded from http://rupress.org/jgp/article-pdf/136/3/325/1788585/jgp_201010454.pdf by guest on 09 February 2026

because CDI should diminish together with SR load). It could also result from a decrease in *B*, also expected, based on the behavior of calsequestrin in aqueous solutions of different $[Ca^{2+}]$ (Park et al., 2003, 2004). Consistent with this explanation, a reduction in buffering power of the SR with SR depletion was demonstrated by Pape et al. (2007), using tetramethyl-murexide to directly monitor $[Ca^{2+}]_{SR}$.

The concentration dependence of Ca^{2+}–calsequestrin binding in aqueous solutions is remarkable for the apparent generation of additional binding sites as $[Ca^{2+}]$ increases. The buffering power, *B*, does not simply grow; interestingly, the "slope" buffering power (Eq. 2) undergoes discrete jumps, apparently associated with successive stages of protein polymerization (Fig. 5 of Park et al., 2004). The present work explored whether this process, operating in reverse, could explain the increase in *E* upon SR depletion. It found that the shoulder of flux and the associated changes in *E* are absent in the cells of double Casq-null mice fully devoid of calsequestrin.

The evaluation of *E* in null mice afforded two separate insights. First, we found that its value (at the time when it can be first equated to the *NFRC* index) was elevated fourfold. Assuming that the initial values of *P* did not change (as indicated by the inability of Casq1 to affect gating of RYR1, demonstrated by Qin et al., 2009, in bilayers), the observed change in *E* would require a fourfold decrease in *B*, implying that calsequestrin provided three fourths of the SR Ca^{2+} buffering at the time of the measurement. (This quantitative estimate would need revising if *P* changed in the null, for example, after alterations in $[Ca^{2+}]_{SR}$, or if the decrease in *B* associated with loss of calsequestrin were offset by "adaptations." Both of these changes are plausible.)

A second insight stems from the observation that the initial value of *E* in the null is close to that reached in the WT by 250 ms into the pulse, when most of the releasable Ca^{2+} is out of the SR (Fig. 3 B). This fact suggests that the decrease in *B* is due to a vanishing contribution of calsequestrin to SR buffering power. This of course implies that the protein inside the SR conserves the behavior described by Park et al. (2003, 2004) for calsequestrin in solution, and, furthermore, that calsequestrin contributes very little as a buffer when $[Ca^{2+}]_{SR}$ is near its minimum.

We tested these inferences by quantifying the response of WT cells with SR depleted in a 0 Ca solution. 15–20 min after cells were placed in 0 Ca, *E* was already greater than in reference solution and continued to increase with time of exposure. Although the time dependence of the effect was variable in different cells, a roughly single-valued inverse functional dependence, plotted in Fig. 6, was found between *E* and releasable amount of SR calcium. The result upholds the hypothesis that the increase in evacuability during long-lasting Ca^{2+} release is

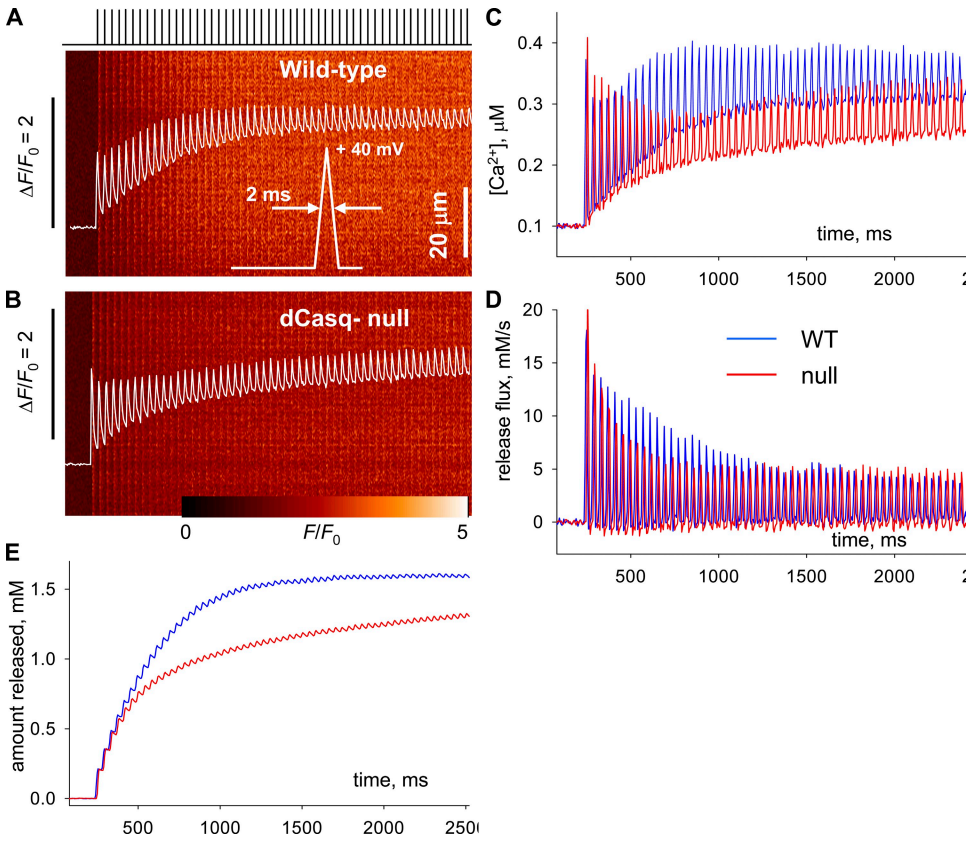

Figure 8. Transients and flux elicited by a pulse train. The figure illustrates the kinetic analysis of Ca^{2+} flux for transients elicited by a train of depolarizing pulses (illustrated in A) to + 40 mV, at 30 Hz, lasting 2.5 s. (A and B) Fluorescence transients in WT and dCasq-null cells. (C and D) Corresponding evolution of $[Ca^{2+}]_{cyto}$ and $\dot{R}_{net}$. (E) Evolution of amount released, $R(t)$. The peaks of the increases in all magnitudes repeat the differences between WT and null illustrated in previous figures. Specifically, fluorescence and $[Ca^{2+}]_{cyto}(t)$ can be compared with the corresponding records in Fig. 2, $\dot{R}_{net}$ and $R(t)$ with those in Fig. 7. ID: WT, 012809b_10; null, 020509b_8.

Downloaded from http://rupress.org/jgp/article-pdf/136/3/325/1788585/jgp_201010454.pdf by guest on 09 February 2026

due to a reduction in buffering power of calsequestrin upon SR depletion. This increase in E implies in turn that SR emptying will accelerate as it proceeds.

In sum, there are two clear reasons for the increase in E during depolarization: an increase in P and a decrease in B. The latter appears prominent in light of the present results, as it alone justifies both the greater resting value of E in null cells and its failure to increase with SR depletion. In contrast, the change in P evaluated in frog muscle was minor overall (Pizarro and Ríos, 2004) or required substantial depletion to become sizable (Pape and Carrier, 2002). An additional reason for the increase in P in the null would be the release of an allosteric inhibition by calsequestrin, similar to the effects reported by the cardiac isoform acting on RYR2 (for review see Knollmann et al., 2006; Györke and Terentyev, 2008; Qin et al., 2008). Such action, however, appears unlikely given the failure of calsequestrin 1 and RYR1 to interact functionally in bilayers (Qin et al., 2009) as their cardiac homologues do.

Implications for the physiological role of calsequestrin

The present results may seem contradictory in their functional implications. On the one hand, they reveal striking changes in the kinetics of Ca^{2+} transients and release flux upon ablation of calsequestrin (Figs. 2 and 4). These alterations, best summarized and quantified by the changes in E, reinforce the consensus that calsequestrin is a substantial Ca^{2+} storage device. Moreover, the unique buffering properties of calsequestrin revealed here are reasonably expected to have virtuous functional consequences.

On the other hand, the results indicate that Casq-null cells are missing only 20% of the releasable calcium, a figure at first sight inconsistent with a central role of the protein in calcium storage. The contractile phenotype of dCasq-null muscle is currently under study and appears generally similar to that of Casq1-null muscle (unpublished data). Therefore the impairments reported here can be compared and are generally consistent with the observations by Paolini et al. (2007) of moderate functional changes in Casq1-null muscle, which include a slowing of the twitch tension transient and a 30% reduction in the calcium transient underlying a twitch. (The present estimate of the difference in releasable calcium, however, is notably smaller than the one offered by Paolini et al., 2007, for Casq1-null cells, who derived it from tension–time integrals in caffeine contractures. The discrepancy could be explained in part by the indirect nature of the tension–time estimate.)

For several reasons, however, the loss of releasable calcium in null animals is likely to underrate the contribution of calsequestrin to the functional reservoir. Note first that net amount released reaches its asymptotic value at 300–500 ms in the WT, but continues to increase in the dCasq-null (Fig. 7 B). Evidently, at long times during a depolarization, the null cells have access to a releasable reservoir that is absent in the WT. This difference could reflect an actual pool of binding sites that is present only in the null. In this regard, the evidence is inconclusive. On the one hand, Paolini et al. (2007) found no compensatory changes in Ca^{2+}-binding proteins reported for the Casq1-null. On the other, in both Casq1-null skeletal fibers and Casq2-null cardiac myocytes the junctional membrane area was increased. If these changes were present in the double null, the lipid membrane itself, or some SR-lumenal molecule associated with it, could provide a greater storage compartment. Alternatively, the newly available pool might consist of binding sites that remain saturated by Ca^{2+} in the WT but become "exposed" in the null, perhaps because $[Ca^{2+}]_{SR}$ decreases further during depolarization in these mice.

Perhaps concurrently, as proposed by Murphy et al. (2009), resting $[Ca^{2+}]_{SR}$ could be increased in the null cells. The SR content of the predominantly fast-twitch cells of rat EDL is far from maximal (Lamb et al., 2001). This observation suggests that the "set point" of free $[Ca^{2+}]_{SR}$ in the predominantly fast-twitch FDB may be well below saturation of calsequestrin in the WT and change in the null mice. A $[Ca^{2+}]_{SR}$ that is higher at rest and decays farther in the nulls could put other buffers into play and explain that releasable calcium remains sizable in the absence of calsequestrin.

A second reason for the presence of large initial release flux in some of the null cells may be a greater number of RYRs, which were overexpressed significantly in Casq1-null cells, matching the increase in area of junctional SR (Paolini et al., 2007).

The study of Knollmann et al. (2006) noted an increase in the volume of the SR of Casq2-null cardiomyocytes and used it to justify in part the apparent lack of consequences of the ablation of calsequestrin for their ability to store and release calcium. This is not the case in Casq1-null skeletal muscle, where there is shrinkage of SR terminal cisternae and no change in total SR volume (Paolini et al., 2007). Moreover, in mouse EDL, the volume of the SR is 5.5% of the cell volume (Eisenberg, 1984), and the SR content is sufficient to increase total calcium concentration in the cytosol to between 1 and 5 mM. Therefore, under the assumption that accessible cytosol is 70% of cell volume, total $[Ca^{2+}]$ in the SR must be 13–64 times greater than free $[Ca^{2+}]_{SR}$. Therefore, even doubling the SR volume would not measurably compensate for loss of buffering power in the null cells. Evidently, extrapolations are not warranted between the roles of calsequestrins and the "adaptive" features of the respective calsequestrin-nulls in skeletal and cardiac cells.

The promotion of SOCE, which is expected upon ablation of calsequestrin (Shin et al., 2003), is unlikely to contribute to the $R(\infty)$ of null cells in the present experiments,

Downloaded from http://rupress.org/jgp/article-pdf/136/3/325/1788585/jgp_201010454.pdf by guest on 09 February 2026

as they were conducted in an external solution with 0.5 mM Cd, an ion that in smooth muscle inhibits this pathway by 50% at 10 μM (McElroy et al., 2008).

In summary, the mild reduction of releasable calcium found in null fibers does not reflect the difference in maximal Ca^{2+} storage capabilities. Several changes in the null could contribute to reducing the difference; the alterations could be structural, including greater area of the SR membrane, or functional, such as an increase in resting $[Ca^{2+}]_{SR}$ and/or the degree of depletion achievable by depolarization. A better definition of these changes will require detailed quantification of releasable Ca^{2+} combined with direct measures of $[Ca^{2+}]_{SR}$ in working muscle cells, a prospect made increasingly feasible by recent advances in the monitoring of SR $[Ca^{2+}]$ (Pape et al., 2007; Jiménez-Moreno et al., 2010 or Reggiani et al., 2010).

The present results include the use, illustrated in Fig. 8, of depolarizations copying a train of action potentials. The situation was still not physiological for multiple reasons, most importantly the presence of EGTA, a buffer that does not affect flux directly (e.g., Rengifo et al., 2002) but drastically modifies the Ca^{2+} transients. In spite of these limitations, the experiment is instructive, showing that every difference between the WT and the null observed under continuous depolarizations is qualitatively conserved under trains of pulses. Voltage clamping with a more physiological pipette solution should give valuable information on the roles of calsequestrin in physiological modes of muscle activity, including exercise that leads to fatigue.

More specifically, the experiment shows that the changes in storage capacity and kinetics featured by the dCasq-null cells result in fairly conserved Ca^{2+} transients, especially during the sustained phase after the first few hundred ms of a pulse train. This may help explain why Casq1-null mice maintain muscle function (Paolini et al., 2007) under conditions of sustained activity. The caveat raised in the previous paragraph applies; however, the value of the observation is limited, as it relies on Ca^{2+} transients altered by a foreign buffer.

Physiological implications of the changes in evacuability

The key finding of the present study is that the overall buffering power of the SR decreases upon store depletion due to changes in the buffering power of calsequestrin. Together with indications that the permeability to Ca^{2+} of the SR membrane increases concomitantly, the observations fully explain the increase in *E* reported by Royer et al. (2008). Thus *E* is assured to increase during Ca^{2+} release from the SR by convergence of two disparate mechanisms, one affecting the channel and the other altering the SR buffer, hence changing the driving force for Ca^{2+} release. We suggest that this convergence could be of value for the physiologically contracting muscle. When the cell is driven to depletion by the stimulation pattern, *P* increases to ensure continued flux in spite of the dwindling driving force, while *B* concurrently decreases to sustain the free $[Ca^{2+}]$ in spite of the diminished store. That the SR hastens its emptying when driven to depletion suggests that the actual response takes precedence to the long-term stability of the store. This "self-immolating" feature seems consistent with the intense but sporadic exertion required of fast-twitch muscle.

We thank Robert Fitts, Marquette University, for helpful discussions on muscle control under physiological conditions.

This work is supported by grants from the National Institute of Arthritis and Musculoskeletal and Skin Diseases (AR049184 and AR032808 to E. Ríos, and AR044750 and AR43140 to P.D. Allen), the Heart and Lung Institute (HL88635 to B.C. Knollmann), the Muscular Dystrophy Association of America (to J. Zhou), and Italian Telethon Research Grant GGP08153 (to F. Protasi).

Richard L. Moss served as editor.

Submitted: 16 April 2010
Accepted: 22 July 2010

REFERENCES

Baylor, S.M., and S. Hollingworth. 1988. Fura-2 calcium transients in frog skeletal muscle fibres. *J. Physiol.* 403:151–192.

Baylor, S.M., and S. Hollingworth. 2003. Sarcoplasmic reticulum calcium release compared in slow-twitch and fast-twitch fibres of mouse muscle. *J. Physiol.* 551:125–138. doi:10.1113/jphysiol.2003.041608

Cheng, H., and W.J. Lederer. 2008. Calcium sparks. *Physiol. Rev.* 88:1491–1545. doi:10.1152/physrev.00030.2007

Domeier, T.L., L.A. Blatter, and A.V. Zima. 2009. Alteration of sarcoplasmic reticulum Ca^{2+} release termination by ryanodine receptor sensitization and in heart failure. *J. Physiol.* 587:5197–5209. doi:10.1113/jphysiol.2009.177576

Donoso, P., H. Prieto, and C. Hidalgo. 1995. Luminal calcium regulates calcium release in triads isolated from frog and rabbit skeletal muscle. *Biophys. J.* 68:507–515. doi:10.1016/S0006-3495(95)80212-2

Eisenberg, B.R. 1984. Quantitative ultrastructure of muscle. *In* Handbook of Physiology; Skeletal Muscle. L.D. Peachey, editor. Lippincott Williams & Wilkins, Philadelphia. 73–112.

Györke, S., and D. Terentyev. 2008. Modulation of ryanodine receptor by luminal calcium and accessory proteins in health and cardiac disease. *Cardiovasc. Res.* 77:245–255. doi:10.1093/cvr/cvm038

Ikemoto, N., M. Ronjat, L.G. Mészáros, and M. Koshita. 1989. Postulated role of calsequestrin in the regulation of calcium release from sarcoplasmic reticulum. *Biochemistry.* 28:6764–6771. doi:10.1021/bi00442a033

Jiménez-Moreno, R., Z.M. Wang, M.L. Messi, and O. Delbono. 2010. Sarcoplasmic reticulum Ca^{2+} depletion in adult skeletal muscle fibres measured with the biosensor D1ER. *Pflugers Arch.* 459:725–735. doi:10.1007/s00424-009-0778-4

Jong, D.S., P.C. Pape, S.M. Baylor, and W.K. Chandler. 1995. Calcium inactivation of calcium release in frog cut muscle fibers that contain millimolar EGTA or Fura-2. *J. Gen. Physiol.* 106:337–388. doi:10.1085/jgp.106.2.337

Knollmann, B.C., N. Chopra, T. Hlaing, B. Akin, T. Yang, K. Ettensohn, B.E. Knollmann, K.D. Horton, N.J. Weissman, I. Holinstat, et al. 2006. Casq2 deletion causes sarcoplasmic reticulum volume increase, premature Ca^{2+} release, and catecholaminergic polymorphic ventricular tachycardia. *J. Clin. Invest.* 116:2510–2520.

Downloaded from http://rupress.org/jgp/article-pdf/136/3/325/1788585/jgp_201010454.pdf by guest on 09 February 2026

Lamb, G.D., M.A. Cellini, and D.G. Stephenson. 2001. Different Ca^{2+} releasing action of caffeine and depolarisation in skeletal muscle fibres of the rat. *J. Physiol.* 531:715–728. doi:10.1111/j.1469-7793.2001.0715h.x

Launikonis, B.S., J. Zhou, L. Royer, T.R. Shannon, G. Brum, and E. Ríos. 2005. Confocal imaging of [Ca^{2+}] in cellular organelles by SEER, shifted excitation and emission ratioing of fluorescence. *J. Physiol.* 567:523–543. doi:10.1113/jphysiol.2005.087973

Launikonis, B.S., J. Zhou, L. Royer, T.R. Shannon, G. Brum, and E. Ríos. 2006. Depletion "skraps" and dynamic buffering inside the cellular calcium store. *Proc. Natl. Acad. Sci. USA.* 103:2982–2987. doi:10.1073/pnas.0511252103

Liu, N., N. Rizzi, L. Boveri, and S.G. Priori. 2009. Ryanodine receptor and calsequestrin in arrhythmogenesis: what we have learnt from genetic diseases and transgenic mice. *J. Mol. Cell. Cardiol.* 46:149–159. doi:10.1016/j.yjmcc.2008.10.012

MacLennan, D.H., and R.A. Reithmeier. 1998. Ion tamers. *Nat. Struct. Biol.* 5:409–411. doi:10.1038/nsb0698-409

MacLennan, D.H., and P.T. Wong. 1971. Isolation of a calcium-sequestering protein from sarcoplasmic reticulum. *Proc. Natl. Acad. Sci. USA.* 68:1231–1235. doi:10.1073/pnas.68.6.1231

McElroy, S.P., A.M. Gurney, and R.M. Drummond. 2008. Pharmacological profile of store-operated Ca(2+) entry in intrapulmonary artery smooth muscle cells. *Eur. J. Pharmacol.* 584:10–20. doi:10.1016/j.ejphar.2008.01.018

Melzer, W., E. Ríos, and M.F. Schneider. 1984. Time course of calcium release and removal in skeletal muscle fibers. *Biophys. J.* 45:637–641. doi:10.1016/S0006-3495(84)84203-4

Murphy, R.M., N.T. Larkins, J.P. Mollica, N.A. Beard, and G.D. Lamb. 2009. Calsequestrin content and SERCA determine normal and maximal Ca^{2+} storage levels in sarcoplasmic reticulum of fast- and slow-twitch fibres of rat. *J. Physiol.* 587:443–460. doi:10.1113/jphysiol.2008.163162

Paolini, C., M. Quarta, A. Nori, S. Boncompagni, M. Canato, P. Volpe, P.D. Allen, C. Reggiani, and F. Protasi. 2007. Reorganized stores and impaired calcium handling in skeletal muscle of mice lacking calsequestrin-1. *J. Physiol.* 583:767–784. doi:10.1113/jphysiol.2007.138024

Pape, P.C., and N. Carrier. 2002. Calcium release and intramembranous charge movement in frog skeletal muscle fibres with reduced (< 250 microM) calcium content. *J. Physiol.* 539:253–266. doi:10.1113/jphysiol.2001.012728

Pape, P.C., D.S. Jong, W.K. Chandler, and S.M. Baylor. 1993. Effect of fura-2 on action potential–stimulated calcium release in cut twitch fibers from frog muscle. *J. Gen. Physiol.* 102:295–332. doi:10.1085/jgp.102.2.295

Pape, P.C., D.S. Jong, and W.K. Chandler. 1995. Calcium release and its voltage dependence in frog cut muscle fibers equilibrated with 20 mM EGTA. *J. Gen. Physiol.* 106:259–336. doi:10.1085/jgp.106.2.259

Pape, P.C., K. Fénelon, C.R. Lamboley, and D. Stachura. 2007. Role of calsequestrin evaluated from changes in free and total calcium concentrations in the sarcoplasmic reticulum of frog cut skeletal muscle fibres. *J. Physiol.* 581:319–367. doi:10.1113/jphysiol.2006.126474

Park, H., S. Wu, A.K. Dunker, and C. Kang. 2003. Polymerization of calsequestrin. Implications for Ca^{2+} regulation. *J. Biol. Chem.* 278:16176–16182. doi:10.1074/jbc.M300120200

Park, H., I.Y. Park, E. Kim, B. Youn, K. Fields, A.K. Dunker, and C. Kang. 2004. Comparing skeletal and cardiac calsequestrin structures and their calcium binding: a proposed mechanism for coupled calcium binding and protein polymerization. *J. Biol. Chem.* 279:18026–18033. doi:10.1074/jbc.M311553200

Pizarro, G., and E. Ríos. 2004. How source content determines intracellular Ca^{2+} release kinetics. Simultaneous measurement of [Ca^{2+}] transients and [H^{+}] displacement in skeletal muscle. *J. Gen. Physiol.* 124:239–258. doi:10.1085/jgp.200409071

Qin, J., G. Valle, A. Nani, A. Nori, N. Rizzi, S.G. Priori, P. Volpe, and M. Fill. 2008. Luminal Ca^{2+} regulation of single cardiac ryanodine receptors: insights provided by calsequestrin and its mutants. *J. Gen. Physiol.* 131:325–334. doi:10.1085/jgp.200709907

Qin, J., G. Valle, A. Nani, H. Chen, J. Ramos-Franco, A. Nori, P. Volpe, and M. Fill. 2009. Ryanodine receptor luminal Ca2+ regulation: swapping calsequestrin and channel isoforms. *Biophys. J.* 97:1961–1970. doi:10.1016/j.bpj.2009.07.030

Reggiani, C., M. Canato, M. Scorzeto, M. Giacomello, F. Protasi, and G.J.M. Stienen. 2010. Impact of calsequestrin on the SR calcium concentration in skeletal muscles fibers monitored with a genetically encoded fret based indicator. *Biophys. J.* 98:546a. doi:10.1016/j.bpj.2009.12.2962

Rengifo, J., R. Rosales, A. González, H. Cheng, M.D. Stern, and E. Ríos. 2002. Intracellular Ca(2+) release as irreversible Markov process. *Biophys. J.* 83:2511–2521. doi:10.1016/S0006-3495(02)75262-4

Ríos, E., B.S. Launikonis, L. Royer, G. Brum, and J. Zhou. 2006. The elusive role of store depletion in the control of intracellular calcium release. *J. Muscle Res. Cell Motil.* 27:337–350. doi:10.1007/s10974-006-9082-5

Royer, L., and E. Ríos. 2009. Deconstructing calsequestrin. Complex buffering in the calcium store of skeletal muscle. *J. Physiol.* 587:3101–3111. doi:10.1113/jphysiol.2009.171934

Royer, L., S. Pouvreau, and E. Ríos. 2008. Evolution and modulation of intracellular calcium release during long-lasting, depleting depolarization in mouse muscle. *J. Physiol.* 586:4609–4629. doi:10.1113/jphysiol.2008.157990

Rudolf, R., P.J. Magalhães, and T. Pozzan. 2006. Direct in vivo monitoring of sarcoplasmic reticulum Ca^{2+} and cytosolic cAMP dynamics in mouse skeletal muscle. *J. Cell Biol.* 173:187–193. doi:10.1083/jcb.200601160

Schneider, M.F., and B.J. Simon. 1988. Inactivation of calcium release from the sarcoplasmic reticulum in frog skeletal muscle. *J. Physiol.* 405:727–745.

Schneider, M.F., B.J. Simon, and G. Szucs. 1987. Depletion of calcium from the sarcoplasmic reticulum during calcium release in frog skeletal muscle. *J. Physiol.* 392:167–192.

Schuhmeier, R.P., and W. Melzer. 2004. Voltage-dependent Ca^{2+} fluxes in skeletal myotubes determined using a removal model analysis. *J. Gen. Physiol.* 123:33–51. doi:10.1085/jgp.200308908

Shin, D.W., Z. Pan, E.K. Kim, J.M. Lee, M.B. Bhat, J. Parness, D.H. Kim, and J. Ma. 2003. A retrograde signal from calsequestrin for the regulation of store-operated Ca2+ entry in skeletal muscle. *J. Biol. Chem.* 278:3286–3292. doi:10.1074/jbc.M209045200

Terentyev, D., S. Viatchenko-Karpinski, I. Györke, P. Volpe, S.C. Williams, and S. Györke. 2003. Calsequestrin determines the functional size and stability of cardiac intracellular calcium stores: mechanism for hereditary arrhythmia. *Proc. Natl. Acad. Sci. USA.* 100:11759–11764. doi:10.1073/pnas.1932318100

Ursu, D., R.P. Schuhmeier, and W. Melzer. 2005. Voltage-controlled Ca^{2+} release and entry flux in isolated adult muscle fibres of the mouse. *J. Physiol.* 562:347–365. doi:10.1113/jphysiol.2004.073882

Valle, G., D. Galla, A. Nori, S.G. Priori, S. Gyorke, V. de Filippis, and P. Volpe. 2008. Catecholaminergic polymorphic ventricular tachycardia-related mutations R33Q and L167H alter calcium sensitivity of human cardiac calsequestrin. *Biochem. J.* 413:291–303. doi:10.1042/BJ20080163

Wang, Y., L. Xu, H. Duan, D.A. Pasek, J.P. Eu, and G. Meissner. 2006. Knocking down type 2 but not type 1 calsequestrin reduces calcium sequestration and release in C2C12 skeletal muscle myotubes. *J. Biol. Chem.* 281:15572–15581. doi:10.1074/jbc.M600090200

Wang, Z.M., M.L. Messi, and O. Delbono. 1999. Patch-clamp recording of charge movement, Ca(2+) current, and Ca(2+) transients in adult skeletal muscle fibers. *Biophys. J.* 77:2709–2716. doi:10.1016/S0006-3495(99)77104-3

Downloaded from http://rupress.org/jgp/article-pdf/136/3/325/1788585/jgp_201010454.pdf by guest on 09 February 2026